

Spectroscopic study of nanocomposites based on PANI and carbon nanostructures for pH sensors

Anita Grozdanov¹, Aleksandar Petrovski¹, Maurizio Avella², Perica Paunović^{1*}, Maria E. Errico², Roberto Avolio², Gennaro Gentile², Francesca De Falco², Aleksandar T. Dimitrov¹

¹ Faculty of Technology and Metallurgy, SS Cyril and Methodius University, RudjerBošković, 16, 1000 Skopje, R. Macedonia

² Institute for Polymers, Composites and Biomaterials, National Research Council, Via Campi Flegrei 34, 80078 Pozzuoli, Italy

Received October 30, 2018; Revised January 7, 2019

Nanocomposites of polyaniline (PANI) and two carbon nanostructures – multiwall carbon nanotubes (MWCNTs) and graphene (G) were obtained by electrochemical polymerization. PANI based nanocomposites with different concentration of carbon nanostructures (CNS:1, 2 and 3wt%) as well as with different methods for CNS dispersion in the electrolyte, were synthesized. The interactions among the CNS nanostructures and polyaniline matrix were studied and the results confirmed strong interactions among the quinoidal structure of PANI and both CNS. In order to design nanocomposite sensors, PANI/CNS nanocomposites were directly electro-polymerized on gold wires of screen printed electrodes. Their sensing activity was evaluated through the resistivity changes at different pH.

Keywords: polyaniline, nanocomposites, carbon nanostructures

INTRODUCTION

Conductive organic polymers capable of conducting electricity due to the partial oxidation or reduction (i.e., doping), were proved as a prospective class of materials in many technological applications [1-3]. They possess an extended π -conjugation along the polymer backbone and exhibit semiconducting behavior [4]. Special attention was given to the polyaniline (PANI) due to its good environmental stability, interesting redox behavior, unique electrical and electrochemical properties, low cost/easy synthesis [4-7]. Depending on the oxidation state, polyaniline can be found in five different states, from which the most important is the so called “emeraldine base” as the most conductive form of neat polyaniline. To achieve conductive polyaniline, emeraldine base must be transformed to emeraldine salt. This can be achieved by doping the emeraldine base with some protonic acids [9]. The choice of the dopant depends on the PANI application [5]. In most of the recent studies, it was shown that hydrochloric and sulphuric acids were the best dopants in terms of stability and conductivity of PANI [10, 11].

PANI application was restricted by its poor mechanical properties and low processability. Because of that, scientists worked to find new ways to improve these properties. One of the approaches is the preparation of PANI-based nanocomposites

with carbon nanostructures (CNS). Recently, it was confirmed that PANI mixed with nanoparticles have emerged as a new class of composites, as the resulting materials demonstrated unique synergistic properties [12]. Among the various nanoparticles, carbon based nanomaterials such as multi-walled carbon nanotubes (MWCNT) and graphene (G) are of particular interest because of their exceptional structural and electronic properties [4, 5]. One of the main reason for application of CNS in nanocomposites is their large surface area to volume ratio, their sp^2 hybridized structure able to give the advantage of π - π interactions with electron rich molecules and their high electrical conductivity. Aromatic structures, in general are known to strongly interact with the basal plane of graphitic surfaces via π -stacking [13, 14].

Several publications have been recently focused on PANI/CNS nanocomposites. Zhou *et al.* demonstrated strong interactions in conjugated systems and greatly improved charge-transfer reaction between polyaniline and carbon nanotubes [14]. Kondawar *et al.* discussed the electrical transport properties of PANI/MWCNT nanocomposites [4]. Kim and Huh [15] prepared PANI/MWCNT-polystyrene composite films with increased electrical conductivity over pure PANI. The enhanced conductivity effect was attributed to carbon nanotubes that may act as conducting bridges between PANI (emeraldine salt) domains due to their large aspect ratio and surface area [16, 17]. As

* To whom all correspondence should be sent.

E-mail: pericap@tmf.ukim.edu.mk

concerning graphene, enhanced electrochemical performances of PANI/G nanocomposites over pristine PANI was reported even if in some cases using modified graphene, these performances decreased. Electrical properties and cycling stability were also improved by the obtainment of graphene chemically grafted with PANI. This was attributed to the increased specific surface area and improved electrical conductivity of graphene [18-21]. Also, amine functionalization of graphene induced improvements of the electrical conductivity and the thermal stability of PANI/G composites [19, 22]. These properties were also found dependent on the particle size and morphology of graphene [5]. Regarding the use of PANI based materials and composites for sensor applications, several work have been reported in the last years to elucidate the chemisorption behavior of PANI and the application of PANI composites in sensors, based on various techniques [23-28]. In a previous work, we have reported the electrochemical polymerization of PANI/CNS nanocomposites and the results obtained on their thermal and morphological characterization in view of the use of these materials for the realization of pH sensors [12]. Preliminary sensing activity of PANI/CNS tablets for pH determination was evaluated using the 4 probe method and interesting results were obtained.

The aim of this work was to obtain a detail characterization of the polymer matrix/CNS-interactions in PANI based nanocomposites containing MWCNT and graphene in order to optimize the properties and the stability of the realized systems.

EXPERIMENTAL

PANI/MWCNT and PANI/G nanocomposites were prepared by electrochemical synthesis described elsewhere [12]. The pristine MWCNTs (code 732, purity ~ 95%, external diameter 10 - 40 nm) were used as received from JRC (ISPRA). Graphene was produced in the laboratories of Faculty of Technology and Metallurgy by molten salt electrolysis using highly oriented graphite electrodes [29]. Before the electrolysis, graphene was purified in 10 wt% solution of H₂O₂ for 2 h and further, in concentrated solution of HF (40 wt%) for 1 h. For some compositions (3wt% of MWCNT and 1,2, and 3 wt% of graphene) further samples were obtained by preliminary deposition of the appropriate amount of CNS on the electrode followed by electro-polymerization. The produced composites were doped in 0.1 M HCl for 24 h. Pure PANI was also synthesized in the same experimental conditions.

Direct electro-polymerization of PANI/CNS nanocomposites on gold wires of screen printed electrodes (SPE) was performed using the same experimental conditions described in reference 12.

Characterization of the prepared nanocomposites was performed by Fourier transform infrared (FTIR) spectroscopy in attenuated total reflectance (ATR) mode, UV-VIS and Raman spectroscopy. FTIR-ATR measurements were carried out on a Perkin Elmer – Spectrum 100 machine using 64 scans. UV-VIS absorption spectra were collected using a JASCO V-570 UV-VIS spectrometer, in the range from 200 to 900 nm with scan speed of 200 nm/min. SEM analysis was done using FEI Quanta 200 system at acceleration voltage of 30 kV.

RESULTS AND DISCUSSION

FTIR-ATR spectra of the prepared PANI/MWCNT nanocomposites are shown in Fig. 1, while FTIR-ATR spectra of PANI/G nanocomposites are shown in Fig. 2.

Due to the incorporation of MWCNT and graphene in the PANI polymer matrix, FTIR-ATR spectra showed the shift of different typical adsorption bands [2,3]. The C=C stretching of quinonoid and benzenoid absorptions of the emeraldine salt in PANI and PANI based nanocomposites were observed at about 1570 cm⁻¹ and ~1480cm⁻¹, respectively [3,4].

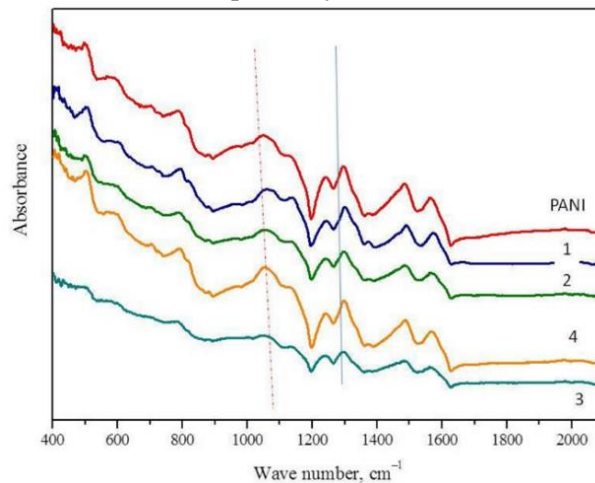


Figure 1. FTIR-ATR spectra of PANI/MWCNT nanocomposites at different MWCNT concentrations: 1) PANI/1 wt% MWCNT; 2) PANI/2 wt% MWCNT; 3) PANI/3 wt% MWCNT, all obtained by preliminary dispersion of MWCNT in the electrolyte; 4) PANI/3 wt% MWCNT obtained after preliminary MWCNT deposition on the electrode. All nanocomposites were obtained with electro-polymerization time of 40 min. FTIR-ATR spectrum of PANI electropolymerized for 40 min is reported for comparison.

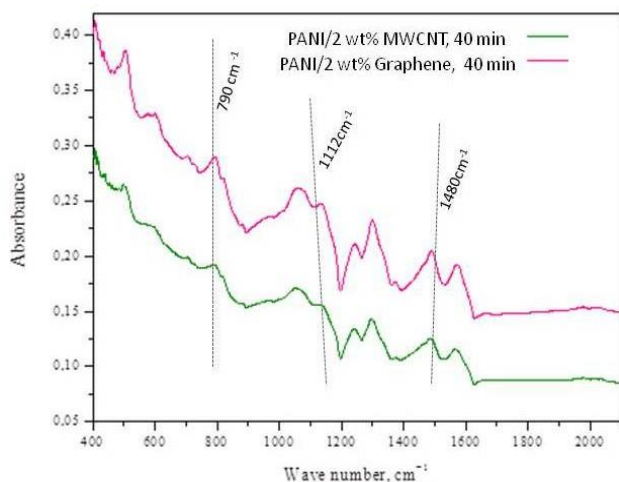


Figure 2. FTIR-ATR spectra of PANI/graphene nanocomposites with different carbon nanostructures (Graphene and MWCNT) with 2 wt% concentrations, all obtained by dispersion of carbon nanostructure in the electrolyte and electropolymerization time of 40 min.

Actually, the characteristic peak at 1560-1630 cm^{-1} attributed to the C=C stretching vibrations of graphite domains of graphene and nanotubes were not clearly detected because of the relatively low amount of CNS and of the overlapping of these absorption bands with the C=C stretching of quinonoid rings of PANI [5]. The C-N stretching and C-H in plane and out-of-plane bending absorption, typical for PANI, were also observed for all the samples at $\sim 1300 \text{ cm}^{-1}$, 1112 cm^{-1} and 790 cm^{-1} , respectively. For all the nanocomposites, either those obtained by dispersion of CNS in the electrolyte, either those obtained by preliminary deposition of the CNS on Pt electrode, the absorption band centered at about 1570 cm^{-1} was shifted to higher wave number values with respect to neat PANI. Moreover, for all the nanocomposite samples, by increasing the concentration of nanostructures from 1 to 3 wt%, the C-N stretching absorption band centered at about 1300 cm^{-1} was shifted to lower values, close to 1290 cm^{-1} [3]. Structural changes obtained by adding CNS to PANI were also evidenced by UV-VIS spectroscopy. Fig. 3 shows the UV-VIS spectra of PANI/MWCNT nanocomposites and Fig. 4 the UV-VIS spectra of PANI/graphene nanocomposites.

The emeraldine form of PANI polymer matrix exhibited two peaks with maxima at about 320 nm, corresponding to $\pi-\pi^*$ transition centered on the benzenoid unit, and about 620 nm, corresponding to the quinonoid excitation band [2]. A shoulder at 272 nm in the PANI spectrum corresponded to $\pi-\pi^*$ transitions of aromatic C-C bonds. A comparison of the effect of the addition of graphene and MWCNT to plain PANI is summarized in Table 1 for nanocomposites containing 2 and 3 wt% of

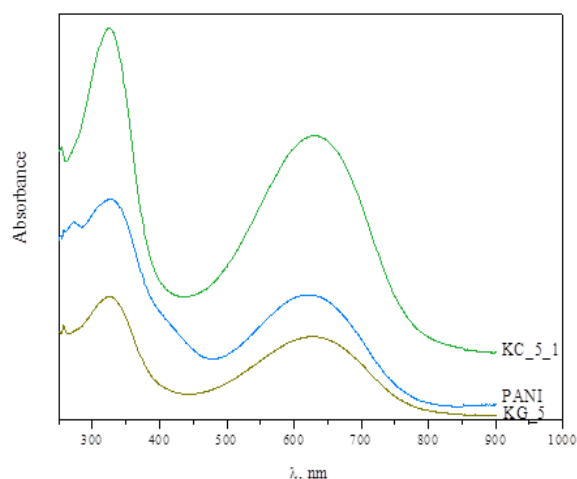


Figure 3. UV-VIS spectra of PANI/3 wt% MWCNT(KC5) and PANI/3 wt% Graphene (KG5) nanocomposites. All nanocomposites were obtained with electro-polymerization time of 40 min. UV-VIS spectrum of PANI electro-polymerized for 40 min is reported for comparison.

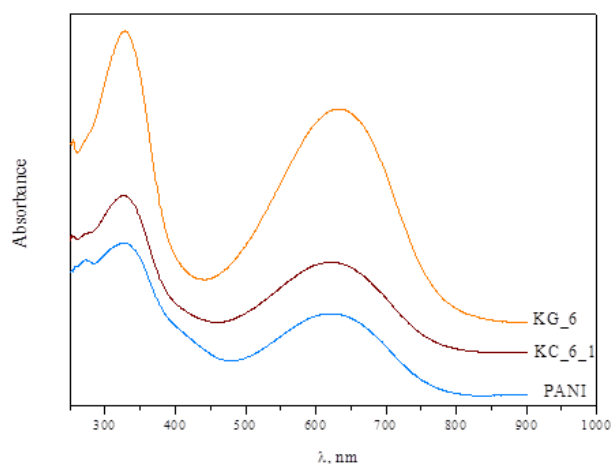


Figure 4. UV-VIS spectra of PANI/2 wt% MWCNT and PANI/2 wt% Graphene nanocomposites. All nanocomposites were obtained with electro-polymerization time of 40 min. UV-VIS spectrum of PANI electro-polymerized for 40 min is reported for comparison.

Table 1. UV-VIS data for the prepared PANI based nanocomposites

Sample	λ , nm	λ , nm	$A_{\text{quin}}/A_{\text{benz}}$
PANI	328	621	0,57
PANI/2wt%MWCNT*	326	630	0,74
PANI/2wt%Graphene	329	635	1,00
PANI/3wt%MWCNT*	325	622	0,4233
PANI/3wt%Graphene	328	634	0,9868

*-Nanocomposites obtained by CNS dispersion in the electrolyte followed by electro-polymerization for 40 min

nanofillers obtained by dispersion of CNS in the electrolyte followed by electro-polymerization. For

almost all nanocomposites, in presence of CNS, the characteristic peak at 620 nm was shifted to higher wavelengths values due to the electronic transition between quinonoid and benzenoid of PANI structures [3]. This effect was always recorded for nanocomposites containing graphene, whereas for nanocomposites containing MWCNT in some cases the shift was negligible (see for instance PANI/3 wt% MWCNT in Table 1). CNS and graphene in particular, also induced a relative increase of the intensity of the absorption band centered at 630 nm with respect to the band centered at about 320 nm. As it can be observed in Table 1, for PANI/2 wt% MWCNT and for PANI/2wt% graphene, the intensity ratio of $A_{\text{quin}}/A_{\text{benz}}$ was found 0.74 to 1.00 respectively and these values are significantly higher than $A_{\text{quin}}/A_{\text{benz}}$ of 0.57 recorded for PANI. Lower increase was recorded at higher CNS loading. For PANI/3 wt% MWCNT the $A_{\text{quin}}/A_{\text{benz}}$ ratio was found comparable to that recorded for PANI, whereas for PANI/3 wt% graphene the $A_{\text{quin}}/A_{\text{benz}}$ ratio was about 0.75. This effect can be attributed to possible agglomeration phenomena of the nanofillers, occurring at higher CNS loadings that reduce PANI/CNS interactions. Comparable effects were also recorded for nanocomposites realized by preliminary deposition of CNS on the electrode followed by PANI electro-polymerization. No significant differences were recorded amongst nanocomposites realized by electro-polymerization lasting 40 min or 60 min.

The characteristic morphology of PANI based nanocomposites is shown in Fig. 5 (for PANI/3 wt% MWCNT system) and Fig. 6 (for PANI/3 wt% Graphene system). It is evident that fibrous and porous morphology was found in both nanocomposite systems which is typical for PANI based nanocomposites.

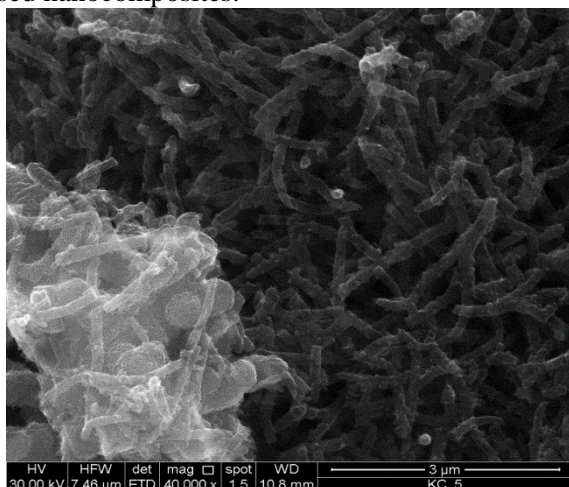


Figure 5. SEM microphotographs of PANI/3 wt% MWCNT.

The high level of interactions established by PANI and CNS in the nanocomposites, confirmed by FTIR, UV-VIS and Raman spectroscopy (Raman analysis published in ref.32), let us suppose a possible significant effect of the nanofillers on the redox properties of PANI in the nanocomposites. Therefore, selected PANI/CNS nanocomposites (PANI/3wt%MWCNT and PANI/3wt%graphene obtained by dispersion of the nanofillers within the electrolyte) were applied on gold SPE by 40 min electro-polymerization. The SPE coated with PANI/MWCNT is exemplificatively shown in the insert in Fig. 7.

Electrical conductivity of these SPE-nanocomposites was measured in different aqueous buffers at various pH values, in order to check the possible suitability of these sensors for pH determination. Interesting, a non linear response was recorded for both MWCNT and graphene nanocomposites coated SPE, with huge electrical resistivity differences recorded at different pH. For instance, the gold SPE coated with PANI/3wt%graphene showed resistivity of 4.60 kΩ.cm at pH=4.5; 360 kΩ.cm at pH=7, and 2430 kΩ.cm at pH=10. A similar trend was also recorded for the gold SPE coated with PANI/3wt%MWCNT. The effect of pH variation on the electrical conductivity of PANI nanocomposites was explained on the basis of different degree of protonation of the imine nitrogen atoms of the polymer chain in the presence of the nanofillers. Starting from these results, further researches are in progress to optimize the composition and the response of the SPE/nanocomposite electrodes.

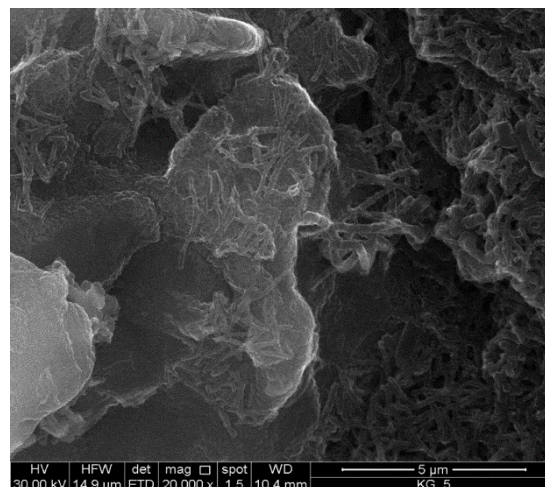


Figure 6. SEM microphotographs of PANI/3 wt% Graphene.

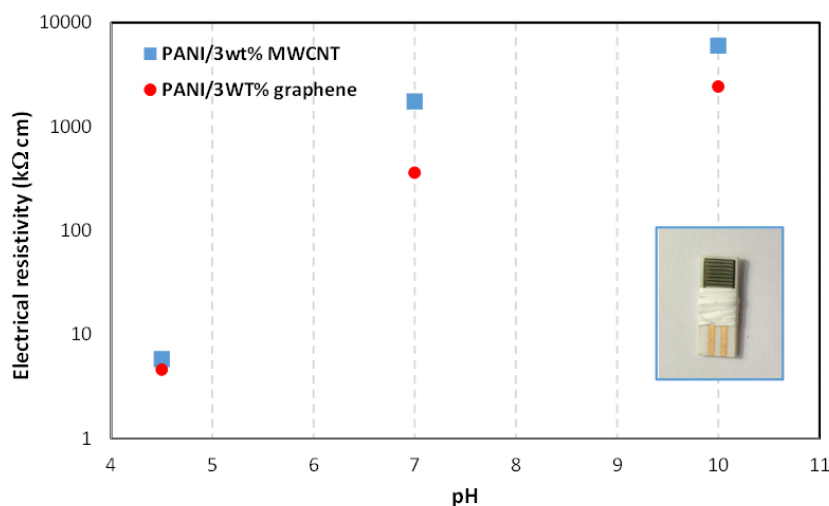


Figure 7. Electrical resistivity of SPE/nanocomposite sensors as a function of pH of aqueous buffer solutions. In the insert, the SPE electropolymerized with PANI/3 wt% MWCNT is shown.

CONCLUSIONS

Characterization of PANI/MWCNT and PANI/graphene nanocomposites prepared by electropolymerization was performed by spectroscopic techniques such as FTIR-ATR, Raman and UV-VIS. The realized nanocomposites were also applied by electro-polymerization on gold SPE and the electrical resistivity of these SPE/nanocomposites was evaluated as a function of the pH of aqueous buffers. Based on the obtained results, the following conclusions were drawn:

Due to the incorporation of pristine MWCNT and graphene nanostructures in the PANI polymer matrix, all spectroscopic analyses indicated strong interactions between the carbon nanostructures and the polymer matrix. In particular, FTIR-ATR spectra showed that for nanocomposites and in particular, for those obtained by preliminary deposition of CNS on the Pt electrode followed by PANI electropolymerization, the typical band of PANI centered at 1571 cm^{-1} was shifted to higher wave number values. The same trend was also the peak attributed to the C–N stretching, centered at about 1300 cm^{-1} , shifted to lower values, down to about $1290\text{--}1294\text{ cm}^{-1}$ by increasing the CNS content in the nanocomposites. Raman spectra of the studied nanocomposites have shown that characteristic bands at 1586 cm^{-1} and 1346 cm^{-1} are due to D peaks and G peaks, respectively, indicating the lattice distortions of the graphene due to the presence of the polyaniline in the network. Also, UV-VIS of nanocomposites were significantly influenced by the presence of CNS, with significant shifts recorded for the peak in comparison to that centered at about 330 nm , in particular in presence of graphene. Raman spectroscopy further confirmed the high

levels of interactions between CNS and PANI, with the significant shift of the position of typical PANI absorption bands and the change of their relative intensity, also in this case more significant for graphene nanocomposites. The electrical behavior of SPE/nanocomposites as a function of the pH of aqueous buffers was evaluated by electrical resistivity measurements. Results were very interesting indicating a non linear dependence of the electrical resistivity with pH, indicating the possible use of these systems for pH determination.

Acknowledgments: This research was performed under the FP7 Project COMMON SENS - "Cost-effective sensors, interoperable with international existing ocean observing systems to meet EU policies requirements" (Project reference 614155).

REFERENCES

1. J. Huang, S. Virji, B. Weiller, R. B. Kaner, *Chem. Eur. J.*, **10**, 1314 (2004)
2. B. J. Gallon, R. W. Kojima, R. B. Kaner, P. L. Diaconescu, *Angew Chem Int Ed Engl.*, **46**, 7251 (2007)
3. V. Gupta, N. Miura, *Mater. Lett.*, **60**, 1466 (2006)
4. S. B. Kondawar, M. D. Deshpande, S. P. Agrawal, *Int. J. Compos. Mater.*, **2**, 32 (2012)
5. R. Arora, A. Srivastav, U. K. Mandal, *Int. J. Mod. Eng. Res. (IJMER)*, **2**, 2384 (2012)
6. H. Shirakawa, E. J. Louis, A. G. MacDiarmid, C. K. Chiang, A. J. Heeger, *J. Chem. Soc., Chem. Commun.*, **16**, 578 (1977)
7. E. Hermelin, J. Petitjean, S. Aeiyaeh, J. C. Lacroix, P. C. Lacaze, *J. Appl. Electrochem.*, **31**, 905 (2001)
8. Y. Wei, G. W. Jang, K. F. Hsueh, E. M. Scherr, A. G. MacDiarmid, A. J. Epstein, *Polymer*, **33**, 314 (1992)
9. D. D. Borole, U. R. Kapadi, P. P. Kumbhar, D. G. Hundiware, *Mater. Lett.*, **57**, 844 (2002)
10. S. H. Kim, J. H. Seong, K. W. Oh, *J. Appl. Polym. Sci.*, **83**, 2245 (2002)

11. A. Pron, J-E. Osterholm, P. Smith, A. J. Heeger, J. Laska, M. Zagorska, *Synth. Met.*, **57** 3520 (1993)
12. A. Petrovski, P. Paunović, R. Avolio, M. E. Errico, M. C. Cocca, G. Gentile, A. Grozdanov, M. Avella, J. Barton, A. T. Dimitrov, *Mater. Chem. Phys.*, **185**, 83 (2017)
13. X-L. Xie, Y-W Mai, X-P. Zhou, *Mater. Sci. Eng. R*, **49**, 89 (2005)
14. Y. Zhou, Z-Y. Qin, L. Li, Y. Zhang, Y-L. Wei, L-F. Wang, M-F. Zhu, *Electrochim. Acta*, **55**, 3904 (2010)
15. W. J. Kim, D. S. Huh, *Bull. Korean Chem. Soc.*, **33**, 2345 (2012)
16. T. M. Wu, Y. W. Lin, *Polymer*, **47**, 3576 (2006)
17. D. K. Kim, K. W. Oh, S. H. Kim, *J. Polym. Sci. Part B Polym. Phys.*, **46**, 2255 (2008)
18. H. K. Hassan, N. F. Atta, A. Galal, *Int. J. Electrochem. Sci.*, **7**, 11161 (2012)
19. S. Sahoo, G. Karthikeyan, G. C. Nayak, C. K. Das, *Macromol. Res.*, **20**, 415 (2012)
20. Z. Gao, F. Wang, J. Chang, D. Wu, X. Wang, X. Wang, F. Xu, S. Gao, K. Jiang, *Electrochim. Acta*, **133**, 325 (2014)
21. J. Li, H. Xie, Y. Li, J. Liu, Z. Li, *J. Power Sources*, **196**, 10775 (2011)
22. S. Sahoo, P. Bhattacharya, G. Hatui, D. Ghosh, C. K. Das, *J. Appl. Polym. Sci.*, **128**, 1476 (2013)
23. Z-F. Li, F. D. Blum, M. F. Bertino, C-S. Kim, *Sens. Actuators B*, **183**, 419 (2013)
24. S. Srivastava, S. S. Sharma, S. Kumar, S. Agrawal, M. Singh, Y. K. Vijay, *Int. J. Hydrogen Energy*, **34**, 8444 (2009)
25. B. Ding, M. Wang, J. Yu, G. Sun, *Sensors*, **9**, 1609 (2009)
26. K. J. Loh, J. P. Lynch, N. A. Kotov, *J. Intell. Mater. Syst. Struct.*, **19**, 747 (2008)
27. Alamusi, N. Hu, H. Fukunaga, S. Atobe, Y. Liu, J. Li, *Sensors*, **11**, 10691 (2011)
28. B. Lakard, G. Herlem, S. Lakard, R. Guyetant, B. Fahys, *Polymer*, **46**, 12233 (2005)
29. A. T. Dimitrov, A. Tomova, A. Grozdanov, O. Popovski, P. Paunović, *J. Solid State Electrochem.*, **17**, 399 (2013)
30. V. Ambrogì, G. Gentile, C. Ducati, M. C. Oliva, C. Carfagna, *Polymer*, **53**, 291 (2012)
31. R. Beams, L. G. Cancado, L. Novotny, *J. Phys. Condens. Mater.*, **27**, 083002 (2015)
32. A. Grozdanov, A. Petrovski, P. Paunovik, A. T. Dimitrov, M. Avella, "MWCNT/Polyaniline Nanocomposites used for pH Nanosensors of Marine waters", pp.231-238, Springer International Publishing AG 2018, M.Cocca et al.(eds.), Proceedings of the International Conference on Microplastic Pollution in the Mediteranean Sea, Springer Water, (2018)https://doi.org/10.1007/978-3-319-71279-6_32